Feedback Gains for Correcting Small Perturbations to Standing Posture

Jiping He, *Member, IEEE,* William S. Levine, *Fellow, IEEE,* and Gerald E. Loeb

Abstract—**A dynamical model of the neuro-musculo-skeletal mechanics of a cat hindlimb has been developed to investigate the feedback regulation of standing posture under small perturbations. The model is a three-joint limb, moving only in the sagittal plane, driven by 10 musculotendon actuators, each having response dynamics dependent on activation kinetics and muscle kinematics. Under small perturbations, the nonlinear postural regulation mechanism is approximately linear. Sensors exist which could provide state feedback. Thus, the linear quadratic regulator is proposed as a model for the structure of the feedback controller for regulation of small perturbations. System states are chosen to correspond to the known outputs of physiological sensors: muscle forces (sensed by tendon organs), a combination of muscle lengths and velocities (sensed by spindle organs), joint angles and velocities (sensed by joint receptors), and motoneuron activities (sensed by Renshaw cells). Thus, the feedback gain matrices computed can be related to the spinal neural circuits. Several proposals for control strategy have been tested under this formulation. It is shown that a strategy of regulating all the states leads to controllers that best mimic the externally measured behavior of real cats.**

I. Introduction

THE use of control theory to provide insight into neurophysiology has a long history. As early as the beginning of the century, Sherrington and his colleagues described stretch reflexes [33], a phenomenon caused by the feedback action of muscle spindles, sensors of a combination of muscle length and rate of change of muscle length.

Most of the previous work on muscle regulation has been based on the theory of single-input single-output (SISO) servomechanisms. An example of particular relevance to our research is Merton's [27] proposal that the stretch reflex was an experimental observation of a motor control strategy, namely, servocontrol of individual muscle length by the spindles. Houk [13] later proposed the regulation of individual muscle stiffness (by sensors of both length and force) as the motor control strategy.

It has recently become possible to trace the sensory feedback pathways through the spinal cord. It is now known that sensory feedback exhibits considerable cross coupling among the actuators [8], [14], [36]. In other words, the neuromuscular control system is certainly multiple-input multiple-output (MIMO).

Because of the enormous number of neurons and reflex pathways involved in the control of locomotion, a comprehensive identification of the structure of the feedback control circuitry is a formidable experimental task. A theoretical approach based on a carefully developed model could shed light on its likely general structure, thereby providing guidance to experimenters. Such a model must consider the mechanical plant consisting of limb segments and musculotendon actuators and the feedback controller, consisting of the reflex pathways in the spinal cord circuitry.

The regulation of static posture and the closely related but more difficult dynamic stabilization of locomotion are rich subjects for theoretical and experimental study. It is quite clear that the highly coupled mechanical structure of the articulated leg [22], [34] and complex dynamics of the musculotendon actuators [37] constitute a complicated nonlinear system.

However, under small perturbations this highly nonlinear but smooth [13] system could be well approximated by a linear system. The applicability of the necessary assumption of linearity depends on the particular system and state being modeled. For example, humans are able to lock their knee joint. If we were linearizing about such a nominal posture, then our linearized model would not include a joint at the knee. However, cats do not lock their knee joint in normal standing. The fact that physiological sensors exist for all of the state variables provides plausibility for a linear state-feedback controller. Thus, a linear quadratic regulator (LQR) is proposed as a model for the neuromuscular regulation of posture. By choosing system states to correspond to physiological sensors, the resulting controller predicts feedback projection patterns of sensory feedback upon spinal interneurons, thus generating some testable hypotheses about interneuronal connections for experimental neuroscientists to investigate.

The feedback gains of the LQR depend on the weighting matrices in the performance criteria. Several possibilities were investigated, including those which correspond to optimal MIMO implementations of both length and stiffness control strategies.

We would be remiss if we did not mention the pioneering paper by Chow and Jacobson [4] which was the first to utilize an LQ model to study human locomotion. Our paper is able to improve, substantially, the relevance to neurophysiology by studying a simpler problem, the regulation of posture, and by utilizing a greatly improved model.

In the next section, we deal with the dynamics of the neuromuscular skeletal control system (NMSCS) and the formulation of the optimization problem. In Section III, we explain the solution of the optimization problem and its relation to the proposed control strategies. In Section IV, we make some connections between the model predictions and experimental data. Finally, we point out some directions for future research.

II. The Model

The NMSCS of a cat hindlimb is a highly efficient locomotion machine. It has been used widely in studies of biomechanics and neurophysiology to understand kinematics and sensorimotor control [15], [16], [21], [32].

Manuscript received March 10, 1989; revised June 7, 1990. Paper recommended by Associate Editor, B. K. Ghosh. This work was supported by the National Institutes of Health under Contracts N01-NS-3-2348 and N01-NS-6-2300.

J. He is with the Center for Biological Information Processing, Massachusetts Institute of Technology, Cambridge, MA 02139.

W. S. Levine is with the Department of Electrical Engineering, University of Maryland, College Park, MD 20742.

G. E. Loeb is with the Biomedical Unit, Abramsky Hall, Queen's University, Kingston, Ont., K7L 3NG, Canada.

IEEE Log Number 9042133.

0018-9286/91/0300-0322$01.00

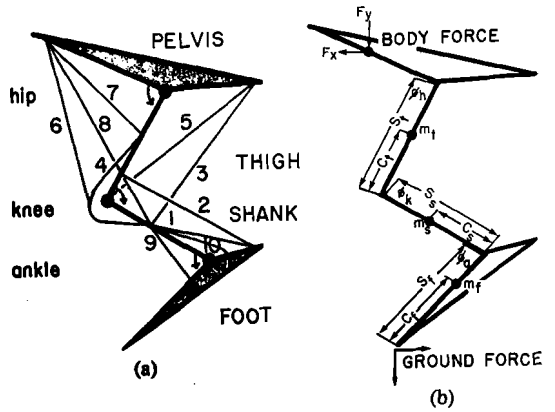

Fig. 1. Definition of musculoskeletal model. (a) Anatomical terms and muscle groups (numbers defined in Appendix, Table III). (b) Corresponding mechanical parameters (values in Appendix, Table I). Abbreviations: S—segment length, m—segment mass, C—center of mass, ϕ—joint angle; subscripts: f—foot, s—shank, t—thigh, a—ankle, k—knee, h—hip.

In this study, a cat hindlimb is modeled in the sagittal plane by a three joint linkage system driven by musculotendon actuators. More than 30 muscles on the limb are grouped into 10 according to their attachment geometries and actions in the sagittal plane. The model preserves the intersegmental coupling and multiarticular muscle structure, but has manageable complexity. The complete model includes four major components: limb mechanics, musculotendon actuators, activation kinetics, and sensors.

A. The Dynamics of the Musculoskeletal Mechanics

Mechanical structures similar to the articulated leg in our model have been studied extensively in both robotics research and biomechanics. Therefore the derivation of the dynamics is omitted. The major differences are in the choice of coordinate systems and the generation of joint torques. We use intersegment joint angles ($(\varphi_h, \varphi_k, \varphi_p)' = \varphi$) as the generalized coordinates. The joint torques are generated by a set of 10 musculotendon actuators. This can be seen from Fig. 1 where the mechanical structure of the system is represented.

The dynamical equations of the system for a standing posture are of the following form:

$$\ddot{\varphi} = J^{-1}(\varphi)\left[M(\varphi, \dot{\varphi}) + N(\varphi)g + \left(\frac{\partial L_p}{\partial \varphi}\right)' F_t + DF_b\right] \quad (1)$$

where

$J(\cdot)$: the moment of inertia matrix;

$M(\cdot)$: the vector of centrifugal and Coriolis forces;

$N(\cdot)$: the coefficients for the gravitational force;

g: the gravitational constant;

$\left(\frac{\partial L_p}{\partial \varphi}\right)'$: the matrix of moment arms for musculotendon actuators. The musculotendon lengths $L_p = (L_{p1}, L_{p2}, \cdots, L_{p10})'$ are determined from the limb configuration and the attachment geometry (see [10] for details);

$F_t = (F_{t1}, F_{t2}, \cdots, F_{t10})'$: the force outputs of the musculotendon actuators;

$F_b = (F_x, F_y)'$: the action of the body on the leg at the hip joint.

$D =$ the matrix of moment arms for F_b.

B. The Dynamics of Musculotendon Actuator

There are several approximations involved in this model. It is clear that cats use their toes to help maintain their balance. However, the forces produced by the muscles that control the toes are relatively small. Modeling the effect of these muscles is very complex because of the many independent articulations involved. Experimental data about toe muscle forces are very difficult to obtain. Thus, the toes have been replaced by a single point-ground contact.

Another major approximation is the assumption that the effect of the other three legs and the rest of the cat's body can be replaced by a force vector at the hip. While this would be unrealistic for many motions it is reasonable for some small perturbations. In particular, it is a reasonable model for experiments in which the contact point of one leg is displaced.

As the actuator, muscle in series with tendon (musculotendon) has always been one of the focal points of motor control research [29], [31]. Surveys of current knowledge about muscle physiology can be found in [7] and [26]. There are many unsettled questions about muscle properties and dynamics, some of which were investigated recently by Rindos [31]. For example, the force–velocity relationship has been studied only during transitions of preactivated muscle from isometric to isokinetic [16] which produces large transients that tend to obscure the more physiologically relevant behavior of muscles activated during isokinetic conditions. Many such complexities in muscle behavior have been reported by experimentalists, but we have modeled only those properties that seem likely to produce large effects under the kinematic conditions of cat locomotion.

In a recent review paper, Zajac presented an excellent summary on modeling the musculotendon actuator [37]. Many forms of dynamical model have been developed to suit different research interests. Most of them are based on the structure shown in Fig. 2. In modeling muscle, it is critically important to define carefully the conditions under which muscles operate. At a standing posture, some muscles are excited to various degrees, while others are completely silent and generate only passive forces when stretched. An applied perturbation of limb position will stretch some muscles while shortening others. This requires a muscle model that can deal simultaneously with both active and passive muscles under all dynamic conditions, that possesses the most relevant properties of musculotendon tissues, and that is simple to use. None of the muscle models found in the literature fully satisfies the requirements because they either need some unobtainable parameters [9] or lose controllability for passive muscles [38]. We modified Zajac's model to deal with the controllability problem while retaining the elegance of the original model. We assumed that all muscles in the model have the same dynamical characteristics and differ only in specific parameters. Hence, parameters in this section are all scalars referring to a general musculotendon actuator.

In solving for the neuromuscular controls to achieve maximum height jumps, Zajac *et al.* [38] assumed a minimum activation ($a(t) \geq a_{\min} > 0$) for all muscles. They assumed that individual muscle mass can be ignored compared to the limb mass being driven and that muscle internal viscosity is negligible. They solved for $\dot{L}_m$ from the relation

$$F_t - F_p \cos \alpha = F_z f_L(L_m) f_V(\dot{L}_m) a \quad (2)$$

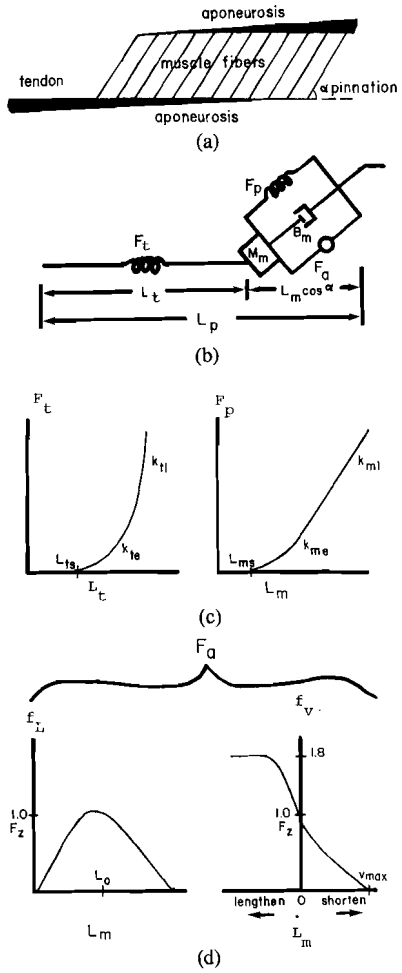

Fig. 2. Definition of muscle model. (a) Anatomical terms. (b) Corresponding mechanical components; L_p—total path length from boney origin to insertion; L_t—combined length of tendon and aponeurotic sheet, which acts as a nonlinear spring to produce force F_t; L_m—length of muscle fascicles; M_m—muscle mass; F_p—force due to parallel elasticity of passive muscle; B_m—parallel viscosity of passive muscle; F_a—force from active force generator. (c) Nonlinear spring stiffness curves for tendon (F_t versus L_t) and passive muscle (F_p versus L_m) showing spring constants k for exponential (subscript e) and linear (subscript 1) terms. (d) Force-length (f_L versus L_t) and force-velocity (f_v versus $\dot{L}_m$) components of active force generator, normalized to maximum isometric force F_z, optimal length L_0 and maximum shortening velocity $v_{\max}$ at zero load. Curves are schematic. They show form but not precise numerical values.

to get

$$\dot{L}_m = f_V^{-1}\left(\frac{F_t - F_p \cos\alpha}{F_z f_L(L_m) a}\right) \tag{3}$$

where

$F_p(F_t, \varphi)$ is the passive force of a muscle due to stretch, and is determined by the musculotendon force F_t and joint angle φ;

F_z is the maximum isometric muscle force the musculotendon actuator can achieve under activation (a constant for each muscle);

$f_L(L_m)$ is the force-length relation of muscle due to myofilament overlap, given in Fig. 2;

$f_V(\dot{L}_m)$ is the force–velocity relation of muscle, an intrinsic property of the crossbridges between the myofilaments that generate the active force as shown in Fig. 2;

$L_m(F_t, \varphi)$ is the relative length of muscle fibers (and hence sarcomeres) which is determined once F_t and φ are given;

$\alpha(F_t, \varphi)$ is the pinnation angle of muscle w.r.t. the action line of F_t, determined by F_t and φ;

$a(t)$ is the mechanical activation level of musculotendon actuator (after motoneuron commands have been transformed by the activation kinetics of the muscle fibers [see (10)]).

The dependence on F_t and φ of F_p, L_m, and α is given by the following equations:

$$F_p = \frac{k_{ml}}{k_{me}}\left(e^{k_{me}(L_m - L_{ms})} - 1\right) \tag{4}$$

$$L_m = \sqrt{L_w^2 + \left(L_p - L_t\right)^2} \tag{5}$$

$$L_t = L_{ts} + \ln\left(k_{te}F_t/k_{tl} + 1\right)/k_{te} \tag{6}$$

$$\cos\alpha = \left(L_p - L_t\right)/L_m \tag{7}$$

where k_i's are spring constants and L_p is the musculotendon length defined earlier.

Substituting $\dot{L}_m$ into the tendon force–length relation gives the dynamics for the musculotendon actuator

$$\dot{F}_t = K_t(F_t)\left[\dot{L}_p - \frac{\dot{L}_m}{\cos\alpha}\right] \tag{8}$$

where $K_t(F_t)$ is the stiffness function of tendon tissues.

This is a model which is computationally tractable yet includes most known propeties of muscle. In reality, however, muscles are often completely relaxed, particularly during slow walking and standing. When $a(t) \to 0$, the aforementioned model is not defined. We have shown elsewhere that it is not always justifiable to ignore muscle mass [10]. Hence, an obvious modification to the model is to include the muscle mass. The corresponding dynamics are given directly by using Newton's laws for the musculotendon actuator shown in Fig. 2 as follows:

$$\ddot{L}_m = \frac{1}{M_m}\left[F_t \cos\alpha - \left(F_z f_L(L_m) f_V(\dot{L}_m) a + F_p + B_m \dot{L}_m\right)\cos^2\alpha\right] + \frac{\dot{L}_m^2 \tan^2\alpha}{L_m}. \tag{9}$$

This generates a two-state representation of the musculotendon actuator. This model can be considered as a general version of many currently available first-order models. For example, the first-order model given earlier can be derived from the model in (9) by applying the technique of singular perturbations, assuming muscle mass to be a small parameter. For detailed derivation and discussion, see [10] and [37].

C. Activation Dynamics

The activation dynamics describes the relation between the neural input to the musculotendon actuator and its mechanical activation. The most important characteristics to be included in the activation dynamics are the different time constants for activation and deactivation, the low-pass filter property, and the saturation of activation. The independence of activation dynamics from muscle contraction dynamics is also assumed [37], although this remains controversial [30].

A first-order nonlinear differential equation is used to describe

the dynamics of activation of the musculotendon actuator

$$\dot{a}(t) = \big(u(t) - a(t)\big)\big(c_1 u(t) + c_2\big) \qquad (10)$$

where u is the neural input (excitation), taken as the rectified smoothed electromyogram (EMG), $c_1 + c_2$ is the activation rate constant (when $u = 1$), and c_2 is the deactivation rate constant (when $u = 0$).

This activation dynamics has the following features.

1) Mechanical activation ($a(t)$) follows excitation ($u(t)$) asymptotically, and is bounded within [0, 1].

2) It has a larger rate constant for activation than deactivation, conforming with the experimental evidence that muscle force rises much faster than it decays.

3) It is an analytical function suitable for feedback control analysis.

D. Physiological Sensors

The limb is equipped with thousands of proprioceptive sense organs whose transduction and encoding properties have been studied intensively. Major physiological sensors considered in our model include muscle receptors and joint receptors. We have considered only the most sensitive and fastest conducting signal sources, presuming these to be most useful for servoregulation.

Among the muscle receptors we have modeled muscle spindle organs sensing muscle kinematics (length and rate of change in length), and Golgi tendon organs sensing muscle force. Spindles reside deep inside muscles and are parallel with the main muscle fibers, thereby experiencing the same stretch as the muscle fibers. There are direct control neurons (γ motoneurons) innervating spindles, to modulate their sensitivity according to the anticipated range of motion. It is clear now that the outputs of spindles go not only to motoneuron pools controlling the same muscle, but also to those controlling other muscles, forming a complex feedback network [23]. The output signals of spindle organs correspond to a nonlinear function of muscle kinematics, i.e., they are sensitive to both muscle lengths and rate of change of length. Furthermore, the nature of this function can be changed dynamically by the γ motoneurons (see [20] and [23]). Since our study is restricted to posture control during small perturbations, a linear combination of the two mechanical inputs (length and velocity) is a reasonable approximation of activity recorded from hindlimb spindles in naturally behaving animals [18], [21]. The effect of active modulation on spindle organs during standing is simulated by a scaling scheme that limits the range of spindle output within [0, 1]:

$$\begin{cases} s_1 \times \delta L_m + s_2 \times \delta \dot{L}_m = & \text{maximum of } \big(\delta L_m + \delta \dot{L}_m\big) \\ s_1 \times \delta L_m = & 0.5 \text{ maximum of } \big(\delta L_m + \delta \dot{L}_m\big). \end{cases} \qquad (11)$$

The sensitivity of tendon organs is not modulated. Their output signals represent simply tensions, influenced little by rates of change of tension. The discharge rate of tendon organs increases monotonically with tension in muscle, though not exactly linearly [23]. It is quite reasonable to assume a linear function for tendon output during standing posture. As for spindles, tendon organs are known to also have a widespread feedback projection through inhibitory interneurons.

Fig. 3 shows a schematic diagram for some of the known feedback projections of the muscle receptors. For simplicity, only the connection between neurons of a pair of agonist and antagonist muscles at one joint are drawn, though the real projection pattern is much more diffuse [15], [25].

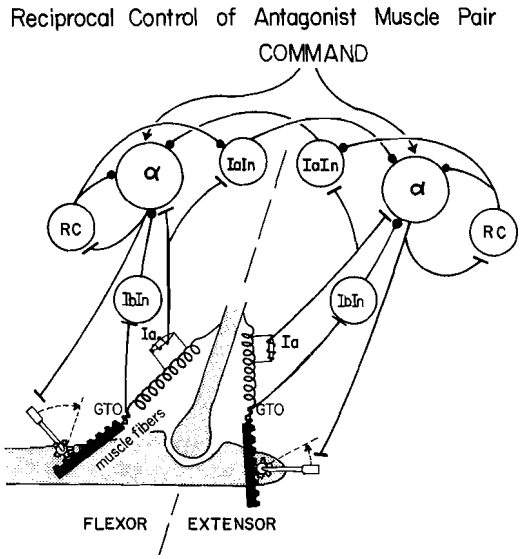

Fig. 3. Classical view of physiological circuitry involved in feedback regulation of muscles acting across a single joint (adapted from [2] and [17]). Large circles denote alpha motoneurons whose excitatory output (bar-shaped endings) caused the muscle to increase its stiffness (ratchet and spring mechanism) and activates the Renshaw cells (RC) which have inhibitory outputs (ball-shaped endings). Muscle length is sensed by spindles (parallel springs) whose primary output (Ia) excites both homonymous (synergist) motoneurons and an inhibitory neuron (IaIn) to the antagonist motoneurons. Muscle force is sensed by Golgi tendon organs (GTO) whose Ib fiber output excites an interneuron (IbIn) that inhibits the homonymous motoneurons. In reality, there are many more convergences on interneurons, including direct input from higher centers that command the motoneurons to increase or decrease muscle activation.

Notice from the figure the connection of a special interneuron —the Renshaw cell (RC). It receives input from a collateral of the axon coming out of the motoneuron and feeds back the signal to both the original motoneuron and to other motoneurons. Neuroscientists have proposed several functions for RC [2]. We believe it is an estimator of muscle activation level, because of the signal it receives and its projection within the spinal cord. Since RC was never considered as a sensor before, no experimental data are available to relate the discharge rate of the neuron to motoneuron activity or muscle activation level.

The functional role of joint receptors has been controversial [5]. Intuitively, some sensors are needed to provide information about joint angles and angular velocities. Joint receptors are natural candidates. However, many experiments indicate that signals from joint receptors occur predominantly at extreme or unusually loaded joint positions [24], leading to speculation that their role in locomotion is to signal readiness for the step phase transition [33]. Since many of those experiments were conducted on anaesthesized animals and results were obtained from some subset of all receptors on a joint, one cannot conclude that joint receptors are not used as joint sensors in a normal sense. We assume in our model the availability of joint angle and angular velocity information from joint receptors. We have also examined the observability of the system without explicit joint receptors. The system is observable [10] so it would be possible to incorporate an estimator for joint angle feedback, based on spindle and tendon organ signals.

In summary, we have incorporated sensors based upon four known receptor modalities: joint receptors ($y_1(\varphi, \dot{\varphi})$) for joint angles and angular velocities; tendon organs ($y_2(F_t)$) for force outputs; spindles ($y_3(L_m, \dot{L}_m)$) for a combination of muscle lengths and velocities; and Renshaw cells ($y_4(a)$) for activation

levels in muscles. These provide for a full-state feedback scheme that can be used to model the feedback projection network residing in the spinal cord for the involuntary control of movement. An alternative to the full-state feedback scheme, incorporating an observer to estimate joint angles and angular rates from signals from the other three sensor modalities, has also been developed (see [10]).

E. The Feedback Structure of the NMSCS

In order to relate our results to the physiology, we chose system inputs to be the neural inputs to musculotendon actuators, and the outputs to be the outputs of the physiological sensors identified previously. A block diagram for the NMSCS dynamics is given in Fig. 4. The feedback pathways have been identified as Ia (muscle spindle primary endings) for muscle length and velocity, Ib (tendon organs) for muscle force, Rc (Renshaw cells) for activation level. Because of the uncertainty of joint receptor action in locomotion control, a switch is shown in the figure to indicate uncertainty whether a joint angle receptor or an estimator is used.

For a standing posture, the system response to a small perturbation will be well represented by a linear system. The behavior of the spinal neural controller for involuntary action should also be close to linear. Under these assumptions, we linearized the system dynamics around a quiet standing posture where the nominal values for all parameters are available from experimental measurement. Let δ denote the variation of a variable from its nominal value. Then the system state vector in the linearized system is given by $x = (\delta\varphi, \delta\dot{\varphi}, \delta F_t, \delta\dot{L}_m, \delta a)'$. The linearized system matrices are

$$A = \begin{pmatrix} 0 & I_{3\times 3} & 0 & 0 & 0 \\ \dfrac{\partial f_1}{\partial x_1} & \dfrac{\partial f_1}{\partial x_2} & \dfrac{\partial f_1}{\partial x_3} & 0 & 0 \\ \dfrac{\partial f_2}{\partial x_1} & \dfrac{\partial f_2}{\partial x_2} & \dfrac{\partial f_2}{\partial x_3} & \dfrac{\partial f_2}{\partial x_4} & 0 \\ \dfrac{\partial f_3}{\partial x_1} & 0 & \dfrac{\partial f_3}{\partial x_3} & \dfrac{\partial f_3}{\partial x_4} & \dfrac{\partial f_3}{\partial x_5} \\ 0 & 0 & 0 & 0 & \dfrac{\partial f_4}{\partial x_5} \end{pmatrix}$$

$$B = \begin{pmatrix} 0 \\ 0 \\ 0 \\ 0 \\ \dfrac{\partial f_4}{\partial u} \end{pmatrix}$$

$$C = \begin{pmatrix} \dfrac{\partial y_1}{\partial x_1} & \dfrac{\partial y_1}{\partial x_2} & 0 & 0 & 0 \\ 0 & 0 & \dfrac{\partial y_2}{\partial x_3} & 0 & 0 \\ \dfrac{\partial y_3}{\partial x_1} & 0 & \dfrac{\partial y_3}{\partial x_3} & \dfrac{\partial y_3}{\partial x_4} & 0 \\ 0 & 0 & 0 & 0 & \dfrac{\partial y_1}{\partial x_1} \end{pmatrix}$$

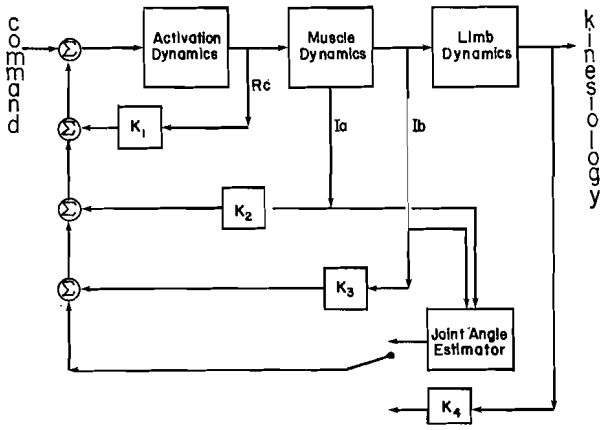

Fig. 4. Block diagram of the neuromusculoskeletal system showing sensorimotor feedback matrix K separated into terms related to state variables for muscle activation (assumed to be sensed by Renshaw cells Rc), muscle length and velocity (spindle Ia afferents) and force (Golgi tendon organ Ib afferents), and joint angle and velocity (either sensed by joint afferents or estimated from Ia and Ib signals).

where f_1 is the skeletal dynamics (1), f_2 is the tendon dynamics (8), f_3 the muscle dynamics (9), and f_4 the activation dynamics (10). Consequently, $A \in R^{36\times 36}$, $B \in R^{36\times 10}$, $C \in R^{33\times 36}$.

To find the linear feedback controller, we assumed a linear quadratic regulator. The performance index to be optimized has the form:

$$J(u) = \frac{1}{2}\int_0^\infty (x'Qx + u'Ru)\,dt. \tag{12}$$

This formulation provides us with two weighting matrices. In effect, at this point the problem is an inverse optimal control problem. Given that the control is linear state feedback, what are the Q and R for which this feedback is optimal?

As an important principle of neuromuscular organization, each muscle fiber receives innervation from only one motoneuron, and one motoneuron can innervate many fibers of the same muscle [3], [26]. We have also assumed that muscle activation is independent of muscle contraction dynamics. Consequently, muscle excitations are independent of each other. Thus, R is assumed to be a diagonal matrix to reflect the independence of excitations for different muscles. Even though the weighting factor in R for each muscle can be different in accordance to its activity at a specific posture, to concentrate on the investigation of the effects of different assumptions about motor control strategy, we used the same weighting for all muscle excitations. Therefore, R is of the form rI.

The choice of Q matrix is determined by the control strategy to be simulated.

1) Under the "joint position servo" control strategy, what is to be minimized is the error in joint positions

$$x'Qx = \sum_{i=1}^{3} q_i \delta\varphi_i^2. \tag{13}$$

2) Under the "length servo" strategy, the controller should regulate the system in such a way that muscle lengths are maintained at their desired values. Correspondingly

$$x'Qx = \sum_{i=1}^{10} q_i \delta L_{pi}^2 = \sum_{i=1}^{10} q_i \left(\frac{\partial L_{pi}}{\partial \varphi}\delta\varphi\right)^2. \tag{14}$$

3) Under the "muscle stiffness" control strategy, proposed by Houk [13], the controller is to minimize any deviation of muscle stiffness from its nominal value. Since the stiffness of a muscle is defined as the ratio between the change in force and that in length, (F_t/L_m), after linearization, we obtain the following:

$$x'Qx = \sum_{i=1}^{10} q_i^f \delta F_{ti}^2 + q_i^l \delta L_{mi}^2. \tag{15}$$

4) Under the "full-state feedback" control strategy, the controller will modulate, in balance, all the state variables to maintain a good performance

$$x'Qx = \sum_{i=1}^{10} \left(q_i^f \delta F_{ti}^2 + q_i^l \delta L_{mi}^2 + q_i^a \delta a_i^2 \right) + \sum_{i=1}^{3} \left(q_i^\varphi \delta \varphi_i^2 + q_i^{\dot\varphi} \delta \dot\varphi_i^2 \right). \tag{16}$$

III. Results

In the previous section, we set up the model for the NMSCS, linearized it around a nominal standing posture, and formulated the optimization problem. The optimal control for the problem, as is well known, is the solution of the corresponding algebraic Riccati equation (ARE) [1]

$$A'K + KA + Q - KBR^{-1}B'K = 0. \tag{17}$$

The Schur decomposition method [18] is used to find the positive-definite solution of the ARE (it is easy to show that the system is controllable and observable). For each Q matrix listed in the previous section, the feedback gain matrix was calculated for several different values of r to see how the feedback pattern changes under different levels of control effort.

The simulation results are compared to experimental measurements to test the various proposals for motor control strategy. The experimental data are from [32]. A cat standing with one foot on each of four movable force plates, has its posture perturbed by a sudden movement of one plate. The ground reaction forces were measured.

Under full-state feedback and when $r = 1.0$, we obtained a ground reaction force response quite similar to the experimental measurement. The results are shown in Fig. 5. The left column shows the perturbation, the measured ground reaction forces, and the computed ground reaction forces. The right column shows the joint angle responses. The response of joint angles and muscle forces (Fig. 6) looks smooth and reasonable.

Under the same control strategy but for different values of r, we obtained similar joint responses but ground reaction forces differed significantly.

It is clear from Fig. 5 that both the shape and the time of the responses of the model match the experimental data reasonably well. We believe the differences are easily explained. Rushmer *et al.* [32] claim that the doubly humped shear reaction force is primarily due to the inertial response to the perturbation. This seems reasonable. The model response is quantitatively different because the model perturbation is exponential while the experimental perturbation was closer to a constant velocity, starting and ending at the negative peaks in the experimental shear reaction force.

In both the real cat and the model the vertical reaction force is kept close to its initial value for a remarkably long time. We believe the cat is able to maintain this value longer than our model by using its other three legs. Similarly, the cat seems to move to a final posture that is slightly different from its initial posture. We do not allow our model to do this although such a change, as a command from a higher neuronal control center (brain or spinal cord), is included in our overall picture of neural control.

Under the other control strategies, however, we either got

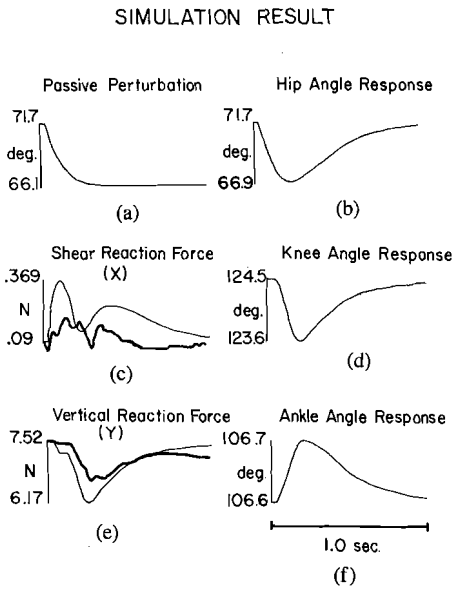

Fig. 5. (a) Simulated response of model system to a small forward perturbation of foot position which produces a small decrease in hip angle that persists in the absence of sensory feedback and (b) is corrected over 1 s as a result of feedback through a matrix that has been optimized for full-state feedback with intermediate level of stiffness; (d) and (f) active corrections at other joints. (c) and (e) Ground reaction forces are compared for simulated response (thin traces) and measured response (thick trace; data traced from [32]).

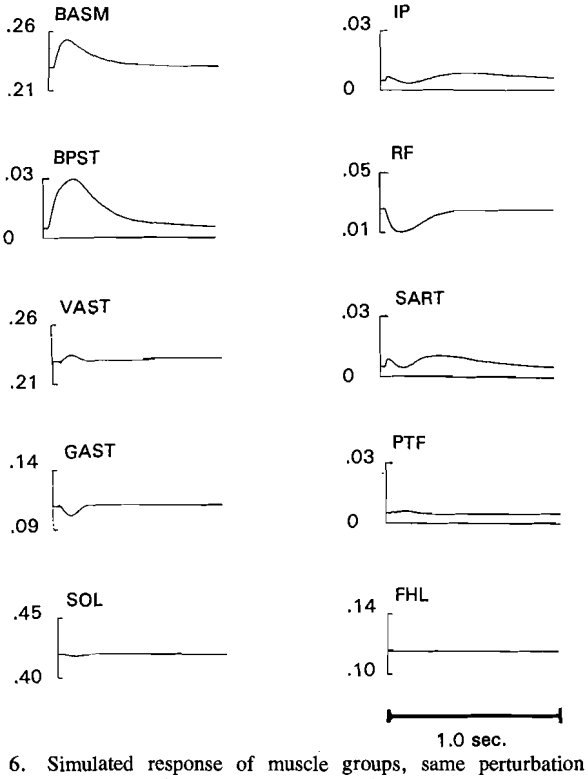

Fig. 6. Simulated response of muscle groups, same perturbation and feedback matrix as in Fig. 5, showing changes in activation (ordinate) over 1 s.

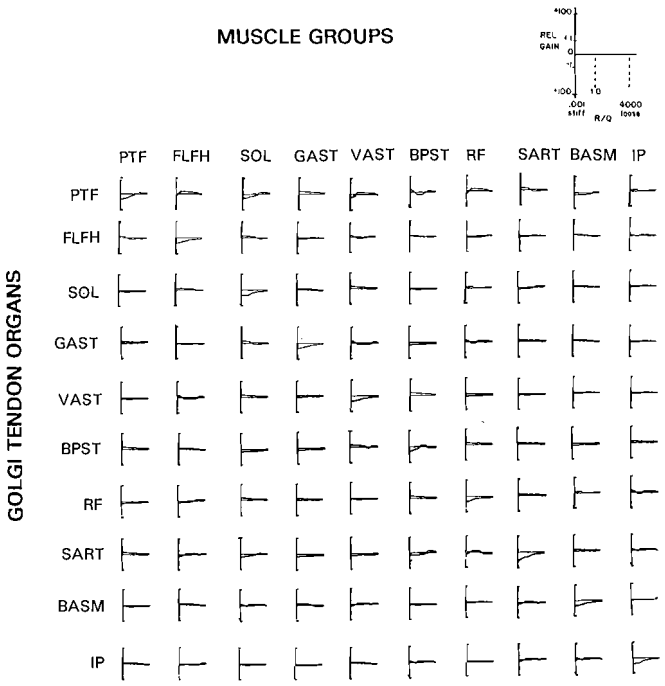

Fig. 7. Portion of feedback matrix K for Golgi tendon organs from all 10 muscle groups (labels on left) onto their controllers (labels at top). Each graph (key upper right) indicates the sign and relative magnitude of feedback gain (ordinate: positive up, pseudologarithmic scale; see text) for a range of performance criteria obtained by varying R/Q ratio (abscissa: log scale from 0.001 to 4000) with full-state feedback.

large force excursions (joint position and length servo control), or large joint angle overshoots (muscle stiffness control). This is evidence that these are not realistic motor control strategies.

These simulations suggest that full state-feedback control might be the motor control strategy used by the NMSCS. The corresponding feedback gain matrix is plotted separately in Fig. 7 for tendon organ feedback projections and in Fig. 8 for spindle organ feedback projections, respectively. Feedback gains for Renshaw cells and joint receptors are not shown here because of the lack of experimental data to give a meaningful discussion.

In Figs. 7 and 8, each small graph represents the feedback gain from one sensor to the control input of one musculotendon actuator as a function of r. The graphs are arranged in columns, according to the neural control input of one musculotendon actuator from all receptors, and in rows, according to the projections of the sensory feedback from one musculotendon actuator to neural control inputs of all actuators.

One pattern that can be immediately recognized from these feedback matrices consists of large excitatory actions (positive feedback) of spindle organs and large inhibitory actions (negative feedback) of tendon organs, on the diagonal elements. These represent the homonymous feedback, of sensors onto the actuators of the same muscles. The signs of these diagonal elements are invariant when r changes, while many heteronymous feedbacks (referring to actions and connections between different muscles) change sign. The pattern from those homonymous feedbacks is consistent with what neurophysiologists have already discovered in experiments. It is this kind of homonymous feedback pattern, and a disregard of the generally smaller heteronymous feedbacks, that prompted proposals for servo control of individual muscles, such as the length servo and muscle stiffness servo. However, there are many heteronymous feedback actions on each muscle, which are not negligible especially when r is large. The simulation suggests that $r = 1.0$ is about the level of control for the NMSCS at standing posture. Around $r = 1.0$, the homonymous actions are still larger than any heteronymous action in all muscles, but the combined effect of the many heteronymous actions on each muscle may be as large or larger.

There are a few exceptions to the homonymous inhibitory action of tendon organs. In Fig. 7, showing tendon organ feedback connections, we can see sign reversals from the homonymous feedback of BPST and PTF. PTF is the major flexor of the ankle joint, while BPST is both a hip extensor and knee flexor. Both muscle groups are silent during quiet standing but the hip flexor RF (which is also a knee extensor) is active. Therefore, the positive force feedback from these two muscle groups might have the effect of increasing the whole limb stiffness in response to the perturbation by temporary cocontraction of both extensors and flexors. These sign reversals of homonymous feedback from BPST and PTF might also have a compensating action for the strong inhibitory feedback of Renshaw cells (not shown) and excitatory action of spindles (Fig. 8) from the same muscles. For MIMO systems, feedback actions are much more complicated, and are no longer as intuitive as they are for SISO systems.

Although heteronymous feedback gains are smaller than homonymous feedback gains, a diffuse feedback projection pattern is generally evident in the feedback matrices. There are feedback connections not only among muscles acting on the same joint, but also acting on different joints. These connections to muscles controlling other joints have a general pattern. The three uniarticular extensors in the model attach to the limb on alternate sides: ankle extensors (*soleus*) on the posterior, knee extensors (*vasti*) on the anterior, and biceps on the posterior of the limb (see Fig. 9). Therefore, the feedback interconnections of the 3 musculotendon actuators also take alternate signs: negative on the ankle, positive on the knee, then negative on the hip. The cat hindlimb is a mechanically coupled multilinkage system with multiarticular musculotendon actuators. We might expect its controller to have comparably distributed structure.

How much is this feedback pattern dependent on the choice of coordinate system used in the model? Let H be a nonsingular transformation matrix relating the new system states z with x. Then we have

$$z = Hx \quad A_x = H^{-1}A_zH \quad B_x = H^{-1}B_z \quad C_x = C_zH.$$

It is easy to show that the relation between the solution of the algebraic Riccati equation under the two coordinate systems is

$$K_x = H'K_zH.$$

From the aforementioned relations, we get

$$G_z = R^{-1}B_z'K_z = R^{-1}B_x'K_xH^{-1} = G_xH^{-1}.$$

Hence, the choice of the system states in the model is important to the generation of the aforementioned feedback patterns, though the control effect will be the same because the optimal control will be

$$u^* = -G_zz = -G_xH^{-1}z = -G_xx.$$

The lesson is that a further aspect to the use of the LQR to model the neurophysiological regulation of posture is the need to infer the appropriate choice of state variables. Fortunately, the well-defined modalities of the naturally occurring sensors correspond well to the natural state variables of a Newtonian model.

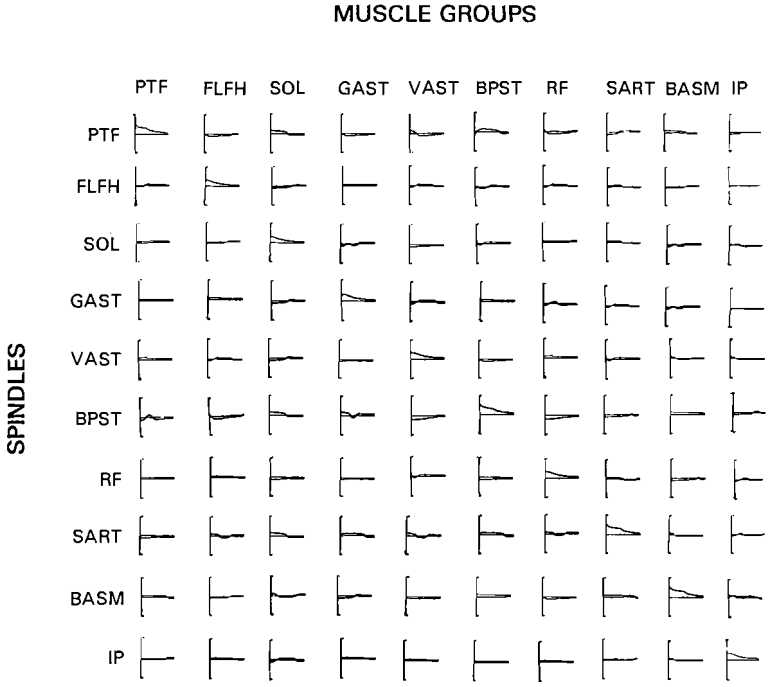

Fig. 8. Portion of feedback matrix K for spindle primary afferents, arranged as in Fig. 7.

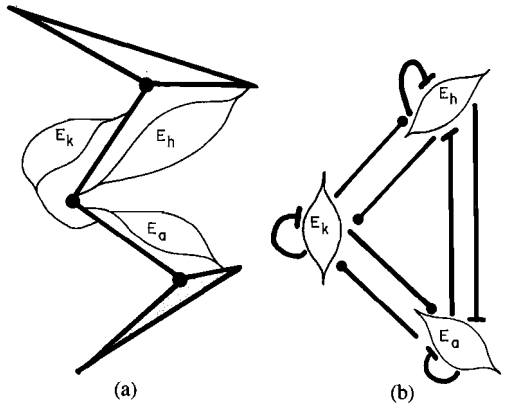

Fig. 9. (a) Anatomical arrangement of monoarticular extensor muscles E of hip h, knee k and ankle a. (b) Corresponding patterns of sensory feedback predicted by optimal regulator design, in which any nominal pattern of homonymous feedback (bar endings looping back onto self) tends to have the reversed sign on muscles operating across the adjacent joint (ball endings) and the same sign for muscles two joints away (bar endings between E_a and E_h).

Because the form of our model retains the essential structure and important physiological properties of the NMSCS, we are able to make some reasonable predictions about neural interconnections of sensory feedback pathways.

However, the neural circuits in the spinal cord are probably much more complex than even those predicted by our LQ control model. After all, we are only describing one specific function of a system with many behaviors. There are many parallel interneuronal systems residing in various reflex pathways, with different latencies. There are additional receptor modalities to those considered in the present model. By using techniques such as neuron staining, microelectrode implantation, and intracellular recording, neurophysiologists have identified extensive heteronymous interconnections and some interneuronal systems in the spinal cord [14], [25]. Because cats are often anaesthesized in such acute experiments, the state of the spinal cord is not known, and there is evidence that the transmission in many such circuits is modulated throughout the different phases of the walking-step cycle. Moreover, because of methodological limitations those acute experiments reveal only the short latency reflex pathways involving one or two interneurons. It is the sum of all contributions from the several parallel interneuronal systems that would generate the net projection strengths that are predicted by this model.

The absolute values of feedback gains depend on the metric used in the model, so we have avoided any interpretation of those values. However, the relative magnitudes of the feedback gains in the matrix constitute important tests of the model's predictions regarding neural connections. If the model prediction is valid, wherever the model predicts small gains there may or may not be a connection; even a strong connection is not a contradiction to our model because the connection might exist, and be used, for an entirely different behavior. If the model predicts a large gain, then there needs to be a strong feedback connection with the appropriate sign to verify our model. The largest gains, which are predicted for homonymous feedback, have long been experimentally established as existing connections in the spinal neural network (Fig. 3), but their relative functional importance during natural motor behaviors remains the subject of study and debate.

The model predicts some reversals in the sign of heteronymous feedback gains, as the ratio of R and Q varies over the range from one extreme to the other. Changes of feedback sign have been observed during the various phases of locomotion in animal experiments [6] and [28]. This suggests, in terms of our model, that the control strategy may change as a function of ongoing motor activity, perhaps as a result of changes in performance criteria, activation state, posture or external constraints (e.g., foot in the air versus on the ground).

VI. Future Research

Since out model contains only one leg of a quadrupedal cat and the motion is restricted to the saggital plane, it is difficult to

TABLE I
SKELETAL SEGMENT DATA, DETERMINED ON FROZEN TRANSECTED LIMB SEGMENTS. ABBREVIATIONS: S—SEGMENT LENGTH (JOINT-CENTER TO JOINT-CENTER); m—SEGMENT MASS (INCLUDING SOFT TISSUE); C—DISTANCE OF CENTER OF MASS FROM THE DISTAL JOINT-CENTER; I—ROTATIONAL MOMENT OF INERTIA (DETERMINED BY PENDULAR OSCILLATION)

Segment	S	m	C	I
	(cm)	(grams)	(cm)	(g cm^2)
Thigh	9.6	234.0	5.7	5353.7
Shank	9.4	54.8	4.4	435.4
Foot	6.9	29.1	3.9	118.5

TABLE II
MUSCLE NAMES, JOINT ACTIONS, AND ATTACHMENT PARAMETERS. ABBREVIATION: H: HIP; K: KNEE; A: ANKLE; E: EXTENSION; F: FLEXION; O1, O2: RANGE OF PROXIMAL ATTACHMENT POINTS; I1, I2: DISTAL ATTACHMENT RANGE. O AND I ARE REPRESENTED AS PERCENTAGE OF THE SEGMENT LENGTH, MEASURED AWAY FROM THE JOINT ACROSS WHICH THE MUSCLE OPERATES

Muscle Name	Joint Action H	K	E	O1 %	O2 %	I1 %	I2 %
Soleus (SOL)	—	—	E	0.6163	0.9249	1.0	
Plantaris (PLA)	—	—	E	0.9356	0.9843	0.2657	
Lateral Gastracnemius (LG)	—	F	E	0.0	0.0849	1.0	
Medial Gastracnemius (MG)	—	F	E	0.0169	0.1213	1.0	
Biceps Posterior (BFP)	E	F	—	1.0		0.33	0.56
Semitendinosus (ST)	E	F	—	1.0		0.2998	0.4763
Gracilis (GRA)	E	F	—	0.3879	1.0	0.2012	0.3668
Tenuissimus (TS)	E	F	—	0.4684		0.5140	
Vastus Intermedius (VI)	—	E	—	0.2779	1.0	0.1584	0.1048
Vastus Medialis (VM)	—	E	—	0.1972	1.0	0.1584	0.1048
Vastus Longus (VL)	—	E	—	0.2779	1.0	0.1584	0.1048
Biceps Anterior (BFA)	E	—	—	1.0		0.0	0.1128
Semimembranosus Longus (SMP)	E	—	—	1.0		0.0507	0.1681
Semimembranosus Brevis (SMA)	E	—	—	1.0		0.7625	1.0
Adductor Femoris (AF)	E	—	—	1.0	0.1222	0.8629	
Caudo Femoralis (CF)	E	—	—	0.1148	0.4592	1.0	
Quado Femoralis (QF)	E	—	—	0.802	1.0	0.085	0.2838
Tensor Fascia Latae Posterior (TFP)	E	—	—	1.0		0.8	
Rectus Femoris (RF)	F	E	—	1.0	0.3947	0.1584	0.1048
Tensor Fascia Latae Anterior (TFA)	F	E	—	0.0		0.1584	0.1048
Sartorius Anterior (SAA)	F	E	—	1.0		0.1584	
Iliopsoas (IP)	F	—	—	0.3797	0.919	0.0769	0.1295
Sartorius Medial (SAM)	F	F	—	1.0	0.823	0.104	0.1135
Tibialis Anterior (TA)	—	—	F	1.0	0.9104	0.3797	
Extensor Digitorum Longus (EDL)	—	—	F	0.95		0.3	
Peroneus Longus (PL)	—	—	F	0.4823	0.8786	0.2342	
Tibialis Posterior (TP)	—	—	E	0.5534	0.8619	0.1996	0.0179
Peroneus Brevis (PB)	—	—	E	0.1028	0.5989	0.3089	0.0185
Flexor Digitorum Longus (FDL)	—	—	E	0.9036		0.2657	
Flexor Hallucis Longus (FHL)	—	—	E	0.1423		0.8635	

make direct comparisons with experimental data other than the ground reaction forces. One obvious improvement is to generalize the model into 3-D space and include more legs. Then the model becomes more complex but more realistic simulation can be performed so that much more experimental data can be used to test the model.

The study of the neural control of walking and running will be more challenging because the dynamical effects become more important in the system behavior. How the neural controller modifies feedback gains to facilitate transitions between different phases of locomotion will be an interesting problem that can be addressed by the approach used here.

Even in the current model, there are still many remaining questions to be answered. The role of joint receptors can be investigated by comparing the patterns of feedback with them or with an estimator for these state variables. Muscle synergy is another issue that can be studied. We have changed Q to test assumptions about motor control strategy. R and Q can also be changed so as to emphasize coordination within selected subgroups of muscles, perhaps incorporating some known features of spinal feedback circuits to determine the relative strength of the "missing," unknown parts of the control system needed to achieve stability.

In summary, the model developed here and the formulation used in its analysis provided us with a tool to study the general structure of the neural control network of the NMSCS. Some experimentally testable predictions were generated and several proposals for motor control strategy were examined. This form of analysis promises to reveal much about the relationship between the neural control circuitry and the musculotendon mechanics.

Please note that we are not claiming that the spinal cord functions as an LQ controller. We are using LQ theory as a tool to study the spinal cord and its relation to the limb. We have

TABLE III

MUSCLE PARAMETERS AND GROUPINGS. ABBREVIATION: PCA: PHYSIOLOGICAL CROSS SECTIONAL AREA; α: MUSCLE FIBER PINNATION ANGLE; L_P: PATHLENGTH (FROM ORIGIN TO INSERTION, INCLUDING TENDON); L_m: MUSCLE FASCICLE LENGTH; EMG: ELECTROMYOGRAM; POE: PEAK OF MUSCLE EXCITATION SEEN IN MAXIMAL EXERTIONS SUCH AS JUMPING AND PAW SHAKING

Group Number Name	Muscle Name	Group Number	PCA cm^2	α deg	L_p cm	L_m cm	Mass g	EMG %POE
1 SOL	SOL	1	0.91	7.0	8.47	4.17	4.03	42
	PLA	1	3.41	14.0	9.77	1.87	6.94	42
2 GAST	LG	2	4.58	17.0	9.54	2.45	12.40	11
	MG	2	4.01	21.0	9.04	2.10	9.60	11
3 BPST	BFP	3	7.55	14.0	9.84	3.69	30.34	0
	ST	3	4.14	0.0	8.02	6.05	12.83	0
	GRA	3	1.34	0.	7.66	6.40	9.41	0
	TS	3						0
4 VAST	VI	4	1.81	7.0	8.37	2.26	4.39	23
	VM	4	2.71	17.0	8.51	2.69	8.39	23
	VL	4	6.51	17.0	9.04	2.73	19.91	23
5 BASM	BFA	5	2.1	14.0	8.46	3.45	12.3	21.6
	SMA	5	1.71	0.0	10.16	8.45	15.33	21.6
	SMP	5	3.43	0.0	10.76	6.20	22.43	21.6
	AF	5	4.98	0.0	11.70	4.86	29.62	21.6
	CF	5	0.6	0.0	11.70	4.86	29.62	21.6
	QF	5						21.6
	TFP	5	0.66	0.0	7.50	3.0	2.06	21.6
6 RF	RF	6	5.41	7.0	9.40	1.92	11.06	2.4
	TFA	6	0.86	9.0	8.9	2.3	2.17	2.4
	SAA	6	1.3	4.2	9.78	8.26	2.98	0
7 IP	IP	7	2.13	0.0	4.3	4.3	1.09	0
8 SART	SAM	8	0.3	0.0	14.4	10.5	9.9	0
9 PTF	TA	9	1.16	7.0	8.9	5.2	6.47	0
	EDL	9	0.95	8.0	9.63	3.36	3.4	0
	PL	9	0.72	7.0	6.15	2.37	1.81	0
10 FLFH	TP	10	1.8	14.0	5.33	0.84	1.65	8.13
	PB	10						8.13
	FDL	10	0.9	10.0	7.4	2.0	1.99	8.13
	FHL	10	4.78	7.0	9.21	1.56	7.93	8.13

used the theory to create a family of models which predict the kinds of feedback that should occur in the spinal cord under precisely stated assumptions.

APPENDIX

CAT HINDLIMB PARAMETERS

Tables I, II, and III provide the parametric data for the musculoskeletal model of the cat hindlimb that was used in the optimal regulator design and simulations of responses to perturbations. These values are a composite of many different specimens used for both morphometric and electromyographical studies. They provide an approximate two-dimensional representation of the state of the system during quiet standing. The optimal regulator designs appear to be relatively robust in the face of small changes in these parameters; systematic sensitivity analysis would shed light on the inherent stability of the system and remains to be done.

ACKNOWLEDGMENT

The authors are grateful to Dr. C. J. Heckman, Dr. C. A. Pratt, Dr. A. J. Rindos, and Dr. J. L. F. Weytjens, for providing valuable data and suggestions.

REFERENCES

[1] M. Athans and P. L. Falb, *Optimal Control.* New York: McGraw-Hill, 1969.

[2] E. Bizzi, N. Accornero, W. Chapple, and N. Hogan, "Arm trajectory formation in monkeys," *Exp. Brain Res.*, vol. 46, pp. 139-143, 1982.

[3] R. Burke and P. Rudomin, "Spinal neurons and synapses," in *Handbook of Physiology—The Nervous Systems I.* Baltimore, MD: Williams and Wilkins, 1981.

[4] C. K. Chow and D. H. Jacobson, "Studies of human locomotion via optimal programming," *Math. Biosci.*, vol. 10, pp. 239-306, 1971.

[5] W. R. Ferrell, S. C. Gandevia, and D. I. Mcloskey, "The role of joint receptors in human kinaesthesia when intramuscular receptors cannot contribute," *J. Physiol.*, vol. 386, pp. 63-71, 1987.

[6] H. Forssberg, "Phasic gating of cutaneous reflexes during locomotion," *Muscle Receptors and Movement*, A. Taylor and A. Prochazka, Eds. Oxford, U.K.: Oxford University Press, 1981.

[7] C. Gans, "Fiber architecture and muscle architecture," *Exerc. Sport Sci. Rev.*, vol. 10, pp. 160-270, 1982.

[8] Z. Hasan and D. G. Stuart, "Animal solutions to problems of movement control: The role of proprioceptors," *Ann. Rev. Neurosci.*, pp. 199-223, 1988.

[9] H. Hatze, "A myocybernetic control model of skeletal muscle," *Biological Cybernetics*, vol. 25, pp. 103-119, 1977.

[10] J. He, "A feedback control analysis of the neuro-musculo-skeletal control system of a cat hindlimb," Ph.D. dissertation, Dep. Elect. Eng., Univ. Maryland, College Park, 1988.

[11] ——, "Partial inversion of cat locomotion dynamics and estimation of joint torques in the left hind limb of a walking cat," M.S. thesis, Dep. Elect. Eng., Univ. Maryland, College Park, MD, 1984.

[12] N. Hogan, "The mechanics of multi-joint posture and movement control," *Biological Cybernetics*, vol. 52, pp. 315-331, 1985.

[13] J. Houk, "Regulation of stiffness by skeletomotor reflexes," *Annual Review of Physiology*, vol. 41, pp. 99-114, 1979.

[14] E. Jankowska, "Interneuronal organization in reflex pathways from proprioceptors," in *Frontiers in Physiological Research.* Australia: Academic Science, 1984.

[15] E. Jankowska, T. Johannisson, and J. Lipski, "Common in-

terneurons in reflex pathways from group Ia and Ib afferents of ankle extensors in the cat," *J. Physiol.*, pp. 381-402, 1981.
[16] G. C. Joyce, P. M. H. Rack, and D. R. Westbury, "The mechanical properties of cat soleus muscle during controlled lengthening and shortening movements," *J. Physiol.*, vol. 204, pp. 461-474, 1969.
[17] E. R. Kandel and J. H. Schwartz, *Principles of Neuroscience*. Amsterdam, The Netherlands: Elsevier, 1984.
[18] A. J. Laub, "A Schur method for solving algebraic Riccati equations," *IEEE Trans. Automat. Contr.*, vol. AC-24, pp. 913-921, 1979.
[19] G. E. Loeb, "The control and responses of mammalian muscle spindles during normally executed motor tasks," *Exercise Sport Sci. Rev.*, vol. 12, pp. 157-204, 1984.
[20] ——, "What the cat's hindlimb tells the cat's spinal cord," in *Feedback and Motor Control in Invertebrates and Vertebrates*, W. Barnes and M. Gladden, Eds. London, U.K.: Croom Helm, 1985.
[21] G. E. Loeb, J. A. Hoffer, and C. A. Pratt, "Activity of spindle afferents from cat anterior thigh muscles,—Part I: Identification and patterns during normal locomotion," *J. Neurophysiology*, vol. 54, no. 3, pp. 549-564, 1985.
[22] G. E. Loeb, W. Marks, A. Rindos, J. He, W. Robert, and W. S. Levine, "The kinematics and dynamics of a cat hindlimb during locomotion," *Soc. Neuroscience Abstr.*, 1985.
[23] P. B. C. Matthews, "Proprioceptors and the regulation of movement," in *Handbook of Behavioral Neurobiology: Motor Coordination*, Vol. 5. New York: Plenum, 1981, ch. 3.
[24] ——, "Where does Sherrington's 'muscular sense' originate? Muscles, joints, corollary discharges?" *Ann. Rev. Neurosci.*, pp. 189-218, 1982.
[25] D. A. McCrea, "Spinal cord circuitry and motor reflexes," *Exercise Sport Sci. Rev.*, vol. 14, pp. 105-141, 1986.
[26] T. A. McMahon, *Muscles, Reflexes, and Locomotion*. Princeton, NJ: Princeton University Press, 1984.
[27] P. A. Merton, "Speculations on the servo control of movement," in *The Spinal Cord*. Boston, MA: Little Brown, 1953.
[28] G. Orlovsky and G. Pavlova, "The effect of different descending systems on flexor and extensor activity during locomotion," *Brain Research*, vol. 40, pp. 359-371, 1972.
[29] P. M. H. Rack, "Limitations of somatosensory feedback in control of posture and movement," in *Handbook of Physiology —The Nervous System II*. Baltimore, MD: Williams and Wilkins, 1981, ch. 7.
[30] P. M. H. Rack and D. R. Westbury, "The effects of length and stimulus rate on tension in the isometric cat soleus muscle," *J. Physiol.*, vol. 204, pp. 443-460, 1969.
[31] A. J. Rindos III, "Determination of muscle force generation by various cat hindlimb muscles under dynamic conditions by means of a computer-automated experimental paradigm," Ph.D. dissertation, Dep. Elect. Eng., Univ. Maryland, College Park, MD, 1988.
[32] D. S. Rushmer, C. J. Russell, J. M. Macpherson, J. O. Phillips, and D. C. Dunbar, "Automatic postural responses in the cat: Responses to headware and tailward translation," *Exp. Brain Res.*, vol. 50, pp. 45-61, 1983.
[33] C. S. Sherrington, "Flexion-reflex of the limb, crossed extension reflex, and reflex stepping and standing," *J. Physiol.*, vol. 40, pp. 28-121, 1910.
[34] J. L. Smith and R. F. Zernicke, "Predictions for neural control based on limb dynamics," *Trends in Neuroscience*, vol. 10, pp. 123-128, 1987.
[35] J. F. Stein, *An Introduction to Neurophysiology*. Oxford, U.K.: Blackwell, 1982.
[36] R. B. Stein, "What muscle variable(s) does the nervous system control in limb movements?" *Behaviorial Brain Sci.*, vol. 5, pp. 535-577, 1982.
[37] F. E. Zajac, "Muscle and tendon: Properties, models, scaling, and application to biomechanics and motor control," *CRC Critical Rev. Biomedical Eng.*, 1988.
[38] F. E. Zajac, W. S. Levine, J. Chapelier, and M. R. Zomlefer, "Neuromuscular and musculoskeletal control models for the human leg," in *Proc. 1983 ACC*, June 1983, pp. 229-234.

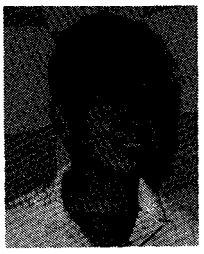

Jiping He (S'86-M'87-S'87-M'88) received the B.S. degree in automatic control engineering from Huazhong University of Science and Technology, Wuhan, China, in 1982 and the M.S. and Ph.D. degrees, in 1985 and 1988, respectively, in electrical engineering, from the University of Maryland, College Park.

From November 1988 to August 1990, he was a postdoctoral fellow at the Artificial Intelligence Laboratory and Brain and Cognitive Sciences, Massachusetts Institute of Technology, Cambridge. He is now an Assistant Professor in the Neurological Surgery Department of Jefferson Medical College of Thomas Jefferson University, and also holds a visiting scientist position in the Department of Mechanical and Aerospace Engineering, Princeton University, Princeton, NJ. His main research interests involve applications of control theory and system engineering to modeling and analysis of sensorimotor control of movement, biomechanics of locomotion, robotics, and nonlinear dynamics.

William S. Levine (S'66-M'68-SM'82-F'86) was born in Brooklyn, NY. He received the B.S., M.S., and Ph.D. degrees from Massachusetts Institute of Technology, Cambridge, in 1962, 1965, and 1969, respectively.

Since 1969, he has been on the faculty of the University of Maryland, College Park, where he is currently Professor of Electrical Engineering and a member of the Systems Research Center. He has also been a consultant for several organizations, including IBM and BTS. His research has been primarily in the applications of control theory to traffic, neurophysiology and control design.

Dr. Levine, J. S. Baras, and T. S. Lin received an award for the outstanding paper in the IEEE TRANSACTIONS ON AUTOMATIC CONTROL for 1978/1979 for "Discrete time point processes in urban traffic queue estimation." He has been working with several collaborators on the control of voluntary movement since 1975. He is presently Editor for *Rapid Publications of Automatica*. He has been an Associate Editor of the IEEE TRANSACTIONS ON AUTOMATIC CONTROL. He was President of the IEEE Control Systems Society in 1990.

Gerald E. Loeb was born in New Brunswick, NJ, on June 26, 1948. He received the B.A. and M.D. degrees from Johns Hopkins University, Baltimore, MD, in 1969 and 1972, respectively.

After completing a surgical internship at the University of Arizona, Tucson, he was a Research Neurophysiologist and Section Chief at the National Institutes of Health in the Laboratory of Neural Control, NINCDS, from 1973 to 1987. Since 1988, he has been Professor of Physiology and Director of Special Projects in the Biomedical Engineering Unit of Queen's University, Kingston, Ont., Canada. He has been involved in many collaborative projects in the field of neural prosthetics, including work on the visual prosthesis at the University of Utah, Salt Lake City, cochlear prostheses at the University of California, San Francisco, and neuromuscular stimulators with the A.E. Mann Foundation of Sylmar, CA.

Dr. Loeb is Chairman of the Biomedical Engineering Committee of the Canadian Medical Research Council and serves on the Editorial Boards of the *Journal of Neurophysiology* and *Exercise and Sport Sciences Reviews*.